nature biomedical engineering

ARTICLES

https://doi.org/10.1038/s41551-018-0293-z

Genome-edited skin epidermal stem cells protect mice from cocaine-seeking behaviour and cocaine overdose

Yuanyuan Li[1,3], Qingyao Kong[2,3], Jiping Yue[1], Xuewen Gou[1], Ming Xu[2*] and Xiaoyang Wu[1*]

Cocaine addiction is associated with compulsive drug seeking, and exposure to the drug or to drug-associated cues leads to relapse, even after long periods of abstention. A variety of pharmacological targets and behavioural interventions have been explored to counteract cocaine addiction, but to date no market-approved medications for treating cocaine addiction or relapse exist, and effective interventions for acute emergencies resulting from cocaine overdose are lacking. We recently demonstrated that skin epidermal stem cells can be readily edited using CRISPR (clustered regularly interspaced short palindromic repeats) and then transplanted back into the donor mice. Here, we show that the transplantation, into mice, of skin cells modified to express an enhanced form of butyrylcholinesterase—an enzyme that hydrolyses cocaine—enables the long-term release of the enzyme and efficiently protects the mice from cocaine-seeking behaviour and cocaine overdose. Cutaneous gene therapy through skin transplants that elicit drug elimination may offer a therapeutic option to address drug abuse.

Drug addiction is a brain disorder characterized by compulsive drug seeking and taking, and a high likelihood of relapse when exposed to drugs or drug-associated cues[1–3]. Cocaine is a commonly abused drug, and current medications do not meet the urgent needs for treating ongoing cocaine use, relapse or acute emergencies that result from cocaine overdose[4,5]. Butyrylcholinesterase (BChE) is a natural enzyme that is present in hepatocytes and plasma, and it hydrolyses its normal substrate acetylcholine[6–8]. BChE can also hydrolyse cocaine at low catalytic efficiency into benzoic acid and ecgonine methyl ester, which are low in toxicity and rewarding properties[9]. Protein engineering has greatly enhanced the catalytic potency and substrate specificity of human BChE (hBChE) for cocaine hydrolysis[10–13]. The modified hBChE has more than 4,400 times higher catalytic efficiency than the wild-type (WT) enzyme with significantly reduced activity for acetylcholine[14]. However, the recombinant hBChE protein has to be delivered via a parenteral route and has a very short half-life in vivo[6,8,15], making it potentially useful only for the acute treatment of cocaine overdose. In recent clinical trials, an hBChE–albumin fusion protein TV-1380 was ineffective in facilitating cocaine abstinence in dependent individuals, probably due to the short half-life of the protein and also the inefficient intramuscular route of injection[16,17]. The development of an ability to stably deliver the engineered hBChE in vivo to allow continuous expression will be highly desirable. Although viral systems have been used for somatic gene delivery, the potential clinical applicability for this approach is greatly limited by the drawbacks of viral vectors, including: strong inflammatory response and tissue toxicity on viral infection; genotoxicity and oncogenic risks of different viral vectors; limited packaging capacities for most viral vectors; and extremely high costs for the preparation of viral stocks at therapeutic grade and quantity[18,19].

Our ex vivo system built on genome-edited skin epidermal stem cells has several unique advantages[20–22], making it particularly suitable for the long-term delivery of hBChE and other effector proteins[20]. (1) As the most accessible organ in the body, the human skin is readily available for extraction of epidermal stem cells through well-established protocols[23–25]. Skin transplants are also easily monitored for potential off-target effects of gene targeting, and removal of skin implants is relatively uncomplicated. (2) Epidermal stem cells can be readily engineered in vitro, and standard procedures exist for transplantation of the differentiated and stratified skin tissue back onto donor patients[26,27]. Compared with viral packaging, autologous skin grafts are inexpensive; skin transplantation is minimally invasive and has been used to treat burn patients for decades[28,29]. (3) Skin epidermal keratinocytes have low immunogenicity as Langerhans cells are the only cell subset that expresses major histocompatibility complex (MHC) class II for antigen-presentation antigens in healthy skin[30]. (4) Other examples of therapeutic large proteins secreted by skin epidermal cells have been reported (for example, apolipoprotein E and the blood clotting factor VIII and factor IX) that can cross the dermal barrier and enter the blood circulation for a systemic therapeutic effect[31–36]. Thus, cutaneous gene therapy can be used as a safe and effective way to treat non-skin diseases including drug abuse—a scenario that has not been explored before. In this report, we demonstrate key evidence that engineered skin transplants can efficiently deliver BChE in vivo and protect against cocaine seeking and overdose.

Results

As the methodology of this study is similar to that in our previous work in ref. [20], some text in this section has been adapted from that publication.

CRISPR-edited epidermal stem cells can express engineered *hBChE* for cocaine hydrolysis. To carry out clustered regularly interspaced short palindromic repeats (CRISPR)-mediated genome editing in mouse epidermal stem cells, we developed DNA vectors encoding the D10A mutant of CRISPR associated protein 9 (*Cas9*^{D10A})[37], two guide RNAs targeting the mouse *Rosa26* locus and a *Rosa26*-targeting vector. The targeting vector contains two

[1]Ben May Department for Cancer Research, University of Chicago, Chicago, IL, USA. [2]Department of Anesthesia and Critical Care, University of Chicago, Chicago, IL, USA. [3]These authors contributed equally: Yuanyuan Li, Qingyao Kong. *e-mail: mxu@dacc.uchicago.edu; xiaoyangwu@uchicago.edu

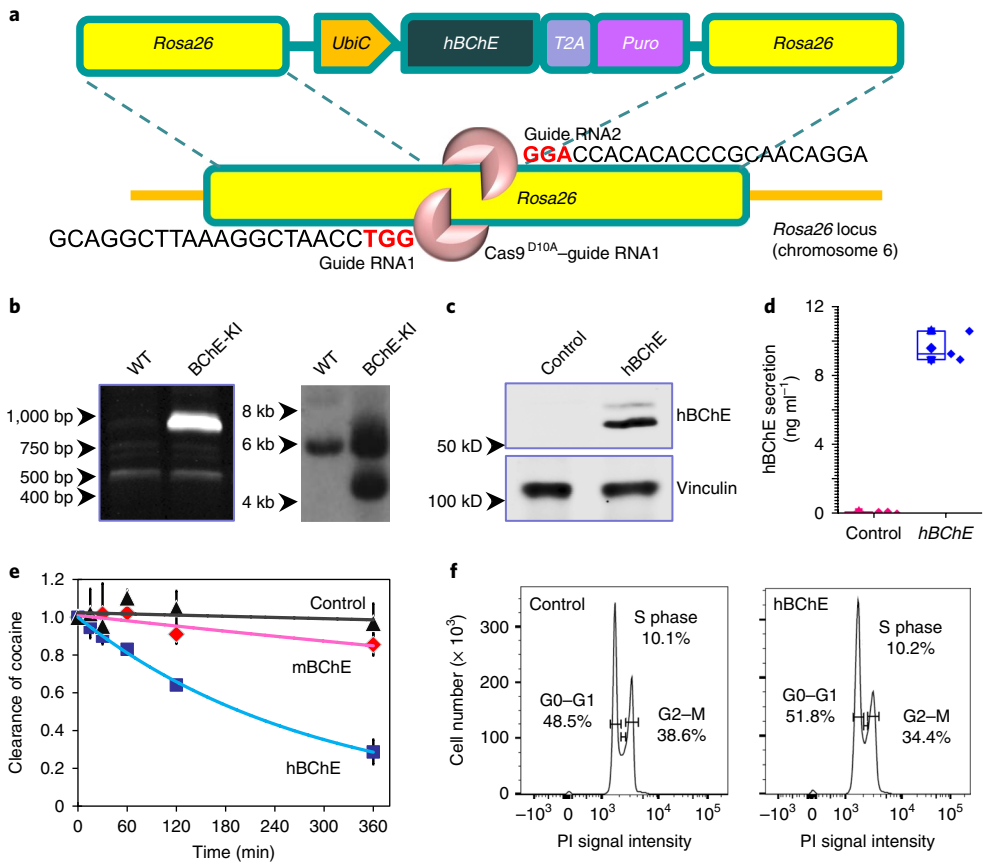

Fig. 1 | Expression of engineered *hBChE* via genome editing in skin epidermal stem cells. a, Targeting strategy for the expression of engineered *hBChE*. The targeting vector contains two *Rosa26* homology arms, which flank the expression cassette for *hBChE* and a selection marker (the puromycin-resistant gene *Puro*) driven by the constitutive promoter ubiquitin C promoter (*UbiC*). *hBChE* and *Puro* are separated by a self-cleavable peptide, *T2A*. **b**, Integration of the targeting vector into the *Rosa26* locus was verified by PCR (left) and Southern blotting (right). Positive clones with *hBChE* integration (BChE-knock-in (KI)) display an additional band of the expected size. Three independent experiments were performed with similar results. bp, base pairs; kb, kilobases. **c**, Confirmation of *hBChE* expression in targeted cells by immunoblots with different antibodies. Numbers to the left indicate molecular weight markers. kD, kilodalton. Full scans of the western blots are provided in Supplementary Fig. 1d. Three independent experiments were performed with similar results. **d**, Confirmation of the secretion of engineered hBChE in the culture media by ELISA. The box plot indicates the mean (solid diamond within the box), 25th percentile (bottom line of the box), median (middle line of the box), 75th percentile (top line of the box), 5th and 95th percentiles (whiskers), 1st and 99th percentiles (solid triangles), and minimum and maximum measurements (solid squares). **e**, Cocaine hydrolysis activity in vitro. Cell culture supernatants were collected from cells targeted by *hBChE* or mouse *BChE* (*mBChE*). Cocaine hydrolysis activity was examined by a clearance assay in vitro. $n = 3$ independent experiments. Error bars represent s.d. and the central measure represents the mean. **f**, Cell cycle profiles of control and *hBChE*-expressing epidermal stem cells. Propidium iodide (PI) was used to identify the proportions of cells that are in various stages of the cell-cycle through flow cytometry and measures of relative DNA content. Three independent experiments were performed with similar results.

homology arms for the *Rosa26* locus, flanking an expression cassette that encodes the modified *hBChE* gene (Fig. 1a). Primary epidermal basal cells were isolated from newborn mice and electroporated with the *Rosa26*-targeting vector together with plasmids encoding *Cas9* and *Rosa26*-specific guide RNAs. Clones were isolated on selection and the correct integration to the *Rosa26* locus was confirmed by both PCR screening and Southern blotting analysis (Fig. 1b). Engineered epidermal cells exhibited robust expression and secretion of hBChE as shown by immunoblots and enzyme-linked immunosorbent assay (ELISA) (Fig. 1c,d). The secreted hBChE protein was functional as the conditioned medium collected from *hBChE*-expressing cells but not the control cells significantly induced degradation of cocaine in vitro (Fig. 1e). Consistent with previous reports, similar mutations in mouse *BChE* lead to only residual activity in cocaine hydrolysis[38] (Fig. 1e). Expression of *hBChE* in epidermal stem cells did not significantly change cell proliferation (Fig. 1f and Supplementary Fig. 1a) or differentiation in vitro (Supplementary Fig. 1b). To confirm that modified epidermal cells are not tumorigenic, we examined the potential anchorage-independent growth of cells. Our results indicated that epidermal stem cells with *hBChE* targeting cannot grow in suspension. In contrast, cancer-initiating cells[39] isolated from mouse squamous cell carcinoma exhibited robust colony-forming efficiency in soft agar medium (Supplementary Fig. 1c).

Engraftment of engineered epidermal stem cells can protect mice from cocaine-seeking behaviour and cocaine overdose. To efficiently transplant mouse epidermal stem cells, we developed an organotypical culture model with mouse epidermal stem cells in vitro by culturing the cells on top of acellularized mouse dermis[20–22]. Exposure to the air–liquid interface can induce stratification of cultured cells to generate a skin-like organoid in vitro. Expression of *hBChE* did not change the ability of epidermal stem cells to stratify (Supplementary Fig. 2a). To investigate the potential therapeutic effect of *hBChE* expression in vivo, we transplanted the organoids to isogenic host animals (CD1 and C57BL/6) (Fig. 2a,b). No significant

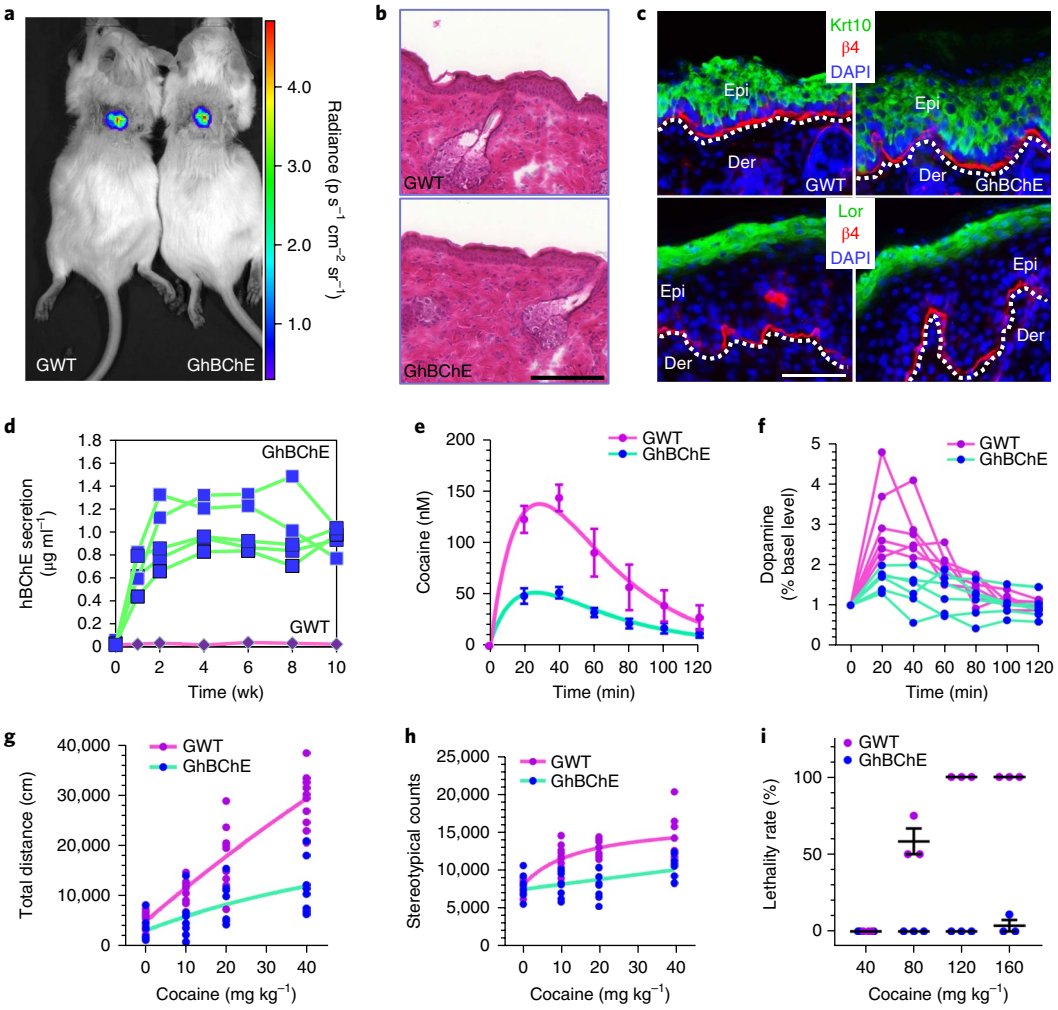

Fig. 2 | Engraftment of *hBChE*-expressing cells can reduce cocaine-induced locomotion and protect against cocaine overdose. a, Skin organoids were developed from control or *hBChE*-producing cells and transplanted to the host mice. Cells were infected with lentivirus encoding firefly luciferase before engraftment to allow intravital imaging of the skin grafts. **b**, Histological examination of grafted skin collected from mice grafted with control (GWT) or *hBChE* skin organoids (GhBChE). Scale bar, 50 μm. **c**, Sections of grafted skin were immunostained with different antibodies (keratin 10 (Krt10), a marker for early epidermal differentiation; loricrin (Lor), a marker for late epidermal differentiation; and β4-integrin (CD104) (β4), a marker for skin basement membrane) as indicated. Dashed lines denote the basement of skin. DAPI, 4′,6-diamidine-2′-phenylindole dihydrochloride; Der, dermis; Epi, epidermis. Scale bar, 50 μm. **d**, Mice were grafted with control (GWT) or *hBChE* skin organoids (GhBChE). The presence of hBChE in the blood was determined by ELISA for 10 wk after engraftment ($n = 5$ mice in each group). **e**, Cocaine pharmacokinetics in the nucleus accumbens after i.p. administration of 10 mg kg^{-1} cocaine in GhBChE and GWT mice ($n = 6$ for each group). Data are plotted as means ± s.e.m. A two-compartment in vivo pharmacokinetic model was built to represent the cocaine concentration–time profile in the nucleus accumbens. **f**, Changes in dopamine levels in the nucleus accumbens after i.p. administration of 10 mg kg^{-1} cocaine in GhBChE and GWT mice ($n = 6$ for each group). Individual lines for each animal were plotted. Treatment × time interaction: $F_{6,70} = 6.549$, $P < 0.0001$, two-way ANOVA. **g**,**h**, Cocaine-induced locomotor activity in GhBChE and GWT mice ($n = 11$ for GWT; $n = 8$ for GhBChE). Non-linear dose versus response curves were simulated to represent cocaine-induced dose–response locomotor activity. **g**, Total distance travelled after 0, 10, 20 and 40 mg kg^{-1} cocaine i.p. injection. Treatment × doses interaction: $F_{3,68} = 11.83$, $P < 0.0001$, two-way ANOVA. **h**, Stereotypical counts after 0, 10, 20 and 40 mg kg^{-1} cocaine i.p. injection. Treatment × doses interaction: $F_{3,65} = 6.223$, $P = 0.0009$, two-way ANOVA. **i**, Lethality rates after injection of 40, 80, 120 and 160 mg kg^{-1} cocaine in GhBChE and GWT mice ($n = 3$ independent experiments; for each experiment, 8 animals were examined in each test group). Individual data points represent the result from each experiment. Error bars represent s.e.m. and the central measure represents the mean.

rejection of the skin grafts was observed for at least five months after transplantation, suggesting that the targeted epidermal stem cells are well tolerated immunologically in vivo. Grafted skin exhibited normal epidermal stratification, proliferation and cell death (Fig. 2c and Supplementary Fig. 2b,c). The mice that were grafted with *hBChE*-expressing cells displayed significant levels of hBChE in the blood (Fig. 2d). Expression of *hBChE* in grafted animals was stable for more than 10 wk (Fig. 2d). Consistent with previous observations[31–36,40], our results confirm that a skin-derived therapeutic protein can cross the basement membrane barrier and enter the circulation in vivo.

Cocaine can block dopamine reuptake and elevate extracellular levels of dopamine, resulting in locomotor stimulation and reward-related behaviours[1,3,41]. The expression of *BChE* in mice grafted with *hBChE*-expressing cells (GhBChE mice) presumably removes cocaine much more quickly in vivo, leading to reduced extracellular dopamine and locomotor activity. We measured dopamine and cocaine levels in both GhBChE mice and control

mice grafted with WT epidermal cells (GWT mice) after an acute cocaine injection. We performed microdialysis in the nucleus accumbens of freely moving mice (Supplementary Fig. 2d), and the dialysates collected were quantified by liquid chromatography–mass spectrometry (LC-MS)[42]. As expected, GhBChE mice exhibited a much faster cocaine clearance (Fig. 2e) and less extracellular dopamine (Fig. 2f) in the nucleus accumbens than WT mice. Consistently, LC-MS analysis demonstrated a significantly faster clearance of benzoylecgonine (a major cocaine metabolite) in the plasma of GhBChE mice (Supplementary Fig. 2e). Engineered hBChE has very low activity for acetylcholine[14]. We did not detect significant differences in plasma acetylcholine levels in GhBChE and control mice (Supplementary Fig. 2f). To further assess the pharmacodynamics properties of cocaine in GhBChE mice, we monitored acute cocaine-induced locomotor behaviour. Both GhBChE and GWT mice exhibited dose–response relationships, as measured by the distance travelled and stereotypical counts, after cocaine administration (Fig. 2g,h). However, GhBChE mice showed significantly less distance travelled and lower stereotypical counts than GWT mice, as revealed by two-way analysis of variance (ANOVA). Together, our data strongly suggest that skin-derived hBChE can effectively hydrolyse cocaine and reduce extracellular levels of dopamine in grafted mice without significant effects on acetylcholine.

To determine whether engrafting hBChE-expressing cells protects mice from the acute systemic toxicity of cocaine, we delivered different doses of cocaine to grafted mice and calculated the lethality rates of cocaine. Doses of 40, 80, 120 and 160 mg kg^{-1} of cocaine had nearly 0 lethality in GhBChE mice, whereas 80 mg kg^{-1} of cocaine induced roughly 50% lethality and 120 and 160 mg kg^{-1} cocaine induced 100% lethality in GWT mice (Fig. 2i and Supplementary Video). A parallel test was conducted to test the toxicity of a related stimulant, methamphetamine, in GhBChE and GWT mice. There was no difference in the lethality induced by various doses of methamphetamine between GhBChE and GWT mice (Supplementary Fig. 2g). This finding suggests that the engraftment of *hBChE*-expressing cells can protect mice from the toxicity of cocaine overdose.

We then assessed protection against the development of cocaine-seeking behaviour using the conditioned place preference (CPP)[43,44] paradigm, which is thought to model reward learning and seeking because experimental animals approach and remain in contact with cues that have been paired with the effects of the reward. We grafted *hBChE*-expressing cells to cocaine-naïve mice and used GWT animals as controls. After 4 d of place conditioning, GWT mice spent significantly more time in environments previously associated with cocaine, whereas GhBChE mice showed no such preference (Fig. 3a). As an additional control, the ethanol CPP was measured after 4 d of conditioning in GhBChE and GWT mice. In contrast, both GhBChE and GWT mice spent significantly more time in ethanol-paired environments (Fig. 3b). This finding indicates that the engraftment of hBChE-expressing cells efficiently and specifically attenuates the cocaine-induced rewarding effect.

To determine whether engrafting hBChE-expressing cells affects cocaine-induced reinstatement of drug seeking, we engrafted *hBChE*-expressing cells in mice that previously acquired cocaine CPP. Following 10 d of recovery, we performed extinction training and drug-elicited reinstatement[43,44]. After a priming dose of cocaine injection, the preference for the previously cocaine-associated environment was restored in the GWT mice but not in the GhBChE mice (Fig. 3c). Because *hBChE* expression did not prevent CPP induction by ethanol (Fig. 3b), we used these GhBChE and GWT mice and performed extinction training followed by reinstatement. In contrast with those induced by cocaine, the ethanol CPP was similarly reinstated in both GhBChE and GWT mice (Fig. 3d). These results suggest that skin-derived hBChE efficiently and specifically disrupts cocaine-elicited reinstatement.

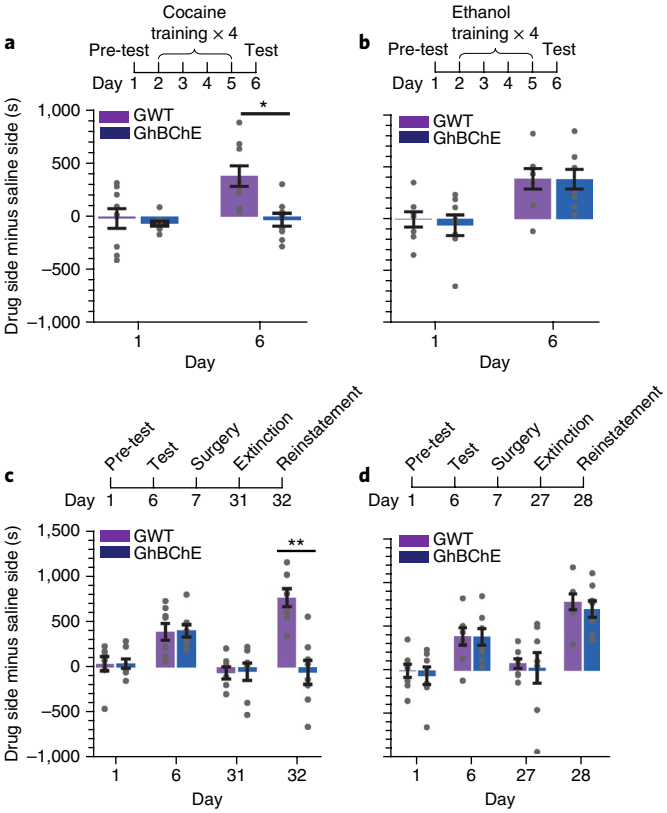

Fig. 3 | Engraftment of *hBChE*-expressing cells can attenuate CPP acquisition and reinstatement induced by cocaine. a, After engraftment, GhBChE and GWT mice underwent pre-testing (day 1), cocaine conditioning (days 2–5) and CPP expression testing (day 6). Data represent means ± s.e.m. ($n = 9$ in each group; treatment × days interaction by repeated-measures ANOVA: $F_{1,16} = 5.04$, $P = 0.039$). Significance was tested by Fisher's least significant difference post hoc test. *$P = 0.016$ between the pre-test and expression test. **b**, After engraftment, GhBChE and GWT mice underwent pre-testing (day 1), ethanol conditioning (days 2–5) and CPP testing (day 6). Data represent means ± s.e.m. ($n = 8$ in each group; treatment × days interaction by repeated-measures ANOVA: $F_{1,14} = 0.084$, $P = 0.76$). **c**, Mice acquired similar levels of cocaine CPP after pre-testing (day 1) and testing after cocaine conditioning (day 6), and underwent engrafting surgery on day 7. Following 10 d of recovery, GhBChE and GWT mice underwent extinction until day 31. During reinstatement on day 32, GhBChE and GWT mice were given a cocaine injection and the CPP was measured again. Data show means ± s.e.m. ($n = 8$ in each group; treatment × days interaction by repeated-measures ANOVA: $F_{3,42} = 12.45$, $P = 6 \times 10^{-6}$). Significance was tested by least significant difference post hoc test. **$P = 0.00013$ between the last extinction and reinstatement. **d**, Mice acquired similar levels of ethanol CPP after pre-testing (day 1) and testing after ethanol conditioning (day 6). They then underwent skin grafting surgery on day 7 and extinction until day 27. During reinstatement on day 28, they were given an ethanol injection and the CPP was recorded. Data show means ± s.e.m. ($n = 8$ in each group; treatment × days interaction by repeated-measures ANOVA: $F_{3,42} = 0.0574$, $P = 0.98$).

Engineered human epidermal stem cells can deliver hBChE in vivo. To test the feasibility of cutaneous gene therapy with human epidermal stem cells, we cultured human skin organoids from primary epidermal keratinocytes isolated from human newborn foreskin. To perform CIRPSR-mediated genome editing in human cells, we developed vectors encoding two guide RNAs targeting the human adeno-associated virus integration site 1 gene (*AAVS1*) locus and an *AAVS1*-targeting vector (Fig. 4a) that harbours the

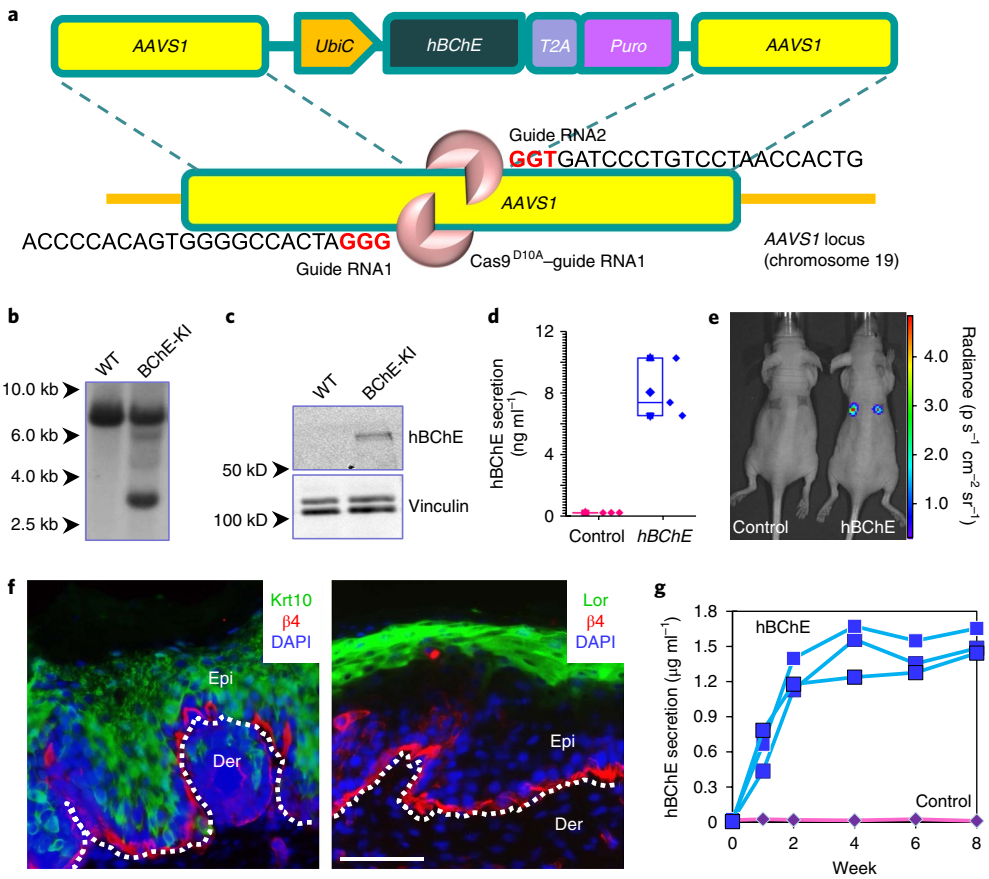

Fig. 4 | Expression of *hBChE* in human epidermal stem cells with CRISPR. a, *AAVS1*-targeting strategy for the expression of engineered *hBChE*. The targeting vector contains two *AAVS1* homology arms, which flank the expression cassette for *hBChE* and a selection marker (the puromycin-resistant gene *Puro*) driven by the constitutive promoter ubiquitin C promoter (*UbiC*). *hBChE* and *Puro* are separated by a self-cleavable peptide, *T2A*. **b**, Integration of the targeting vector into the *AAVS1* locus was verified by Southern blotting. Positive clones with *hBChE* integration (BChE-KI) display an additional band of the expected size. Three independent experiments were performed with similar results. kb, kilobases. **c**, The expression of *hBChE* was confirmed in targeted cells by immunoblots with different antibodies as indicated. Full scans of the western blots are available in Supplementary Fig. 3e. Three independent experiments were performed with similar results. **d**, Secretion of engineered hBChE in the culture media was confirmed by ELISA ($n=3$ independent experiments). Box plots were generated with the same elements as described in Fig. 1d. **e**, Nude mice were grafted with organotypic human skin culture. Intravital imaging shows the efficient incorporation of grafted cells expressing luciferase (right) or control cells (left) on engraftment. **f**, Sections of grafted skin were immunostained with different antibodies (keratin 10 (Krt10), a marker for early epidermal differentiation; loricrin (Lor), a marker for late epidermal differentiation; and β4-integrin (CD104) (β4), a marker for skin basement membrane) as indicated. Dashed lines denote the basement of the skin. Scale bar, 50 μm. DAPI, 4′,6-diamidine-2′-phenylindole dihydrochloride; Der, dermis; Epi, epidermis. **g**, Mice were grafted with control or *hBChE* skin organoids. The presence of hBChE in the blood was determined by ELISA for 8 wk after engraftment ($n=3$ mice per group).

expression cassette encoding engineered *hBChE*. Human epidermal keratinocytes were electroporated with the targeting vector together with plasmids encoding *Cas9* and the guide RNAs. Clones were isolated and the correct integration confirmed by Southern blotting analysis (Fig. 4b). As with mouse cells, engineered human epidermal cells exhibited strong hBChE production, as determined by immunoblots and ELISA (Fig. 4c,d). Expression of the hBChE protein in human cells did not significantly change cell proliferation (Supplementary Fig. 3a) or differentiation (Supplementary Fig. 3b) in vitro. The engineered cells stratified and formed skin organoids in vitro, which were transplanted to nude hosts (Fig. 4e). Grafted skin exhibited normal epidermal stratification, proliferation and apoptosis in vivo (Fig. 4f and Supplementary Fig. 3c,d). Together, these results indicate that CRISPR editing of human epidermal stem cells does not significantly alter cellular dynamics and persistence in vivo. ELISA confirmed that the mice with engraftment of *hBChE*-expressing cells had significant levels of hBChE in the blood, and this expression was stable for more than 8 wk in vivo (Fig. 4g). Our results suggest the potential clinical relevance of cutaneous gene delivery for the treatment of cocaine abuse and overdose in the future.

Discussion

Our study demonstrates that transplantation of genome-edited skin stem cells can be used to deliver an active cocaine hydrolase long term in vivo. Skin epidermal stem cells can be successfully employed for ex vivo gene therapy, as efficient genetic manipulation is possible with minimal risk of tumorigenesis or other adverse events in vivo[31,32]. Skin transplantation protocols, including procedures based on the use of human epidermal stem cells to generate cultured epidermal autografts, have been in clinical use for decades in the treatment of burn wounds[28,29,45]. Engineered skin stem cells and cultured epidermal autografts have also been used to treat other skin diseases, including vitiligo and skin genetic disorders, such as epidermolysis bullosa[46,47]. These regenerated skin grafts are stable and have been shown to survive long term in clinical follow-up studies[29,45–47]. As such, the cutaneous gene therapy is long lasting, minimally invasive and safe. For cocaine addicts and individuals

with a potentially high risk of cocaine abuse who seek help or treatment, the cutaneous gene therapy approach with *hBChE* expression can address several key aspects of drug abuse, including reducing the development of cocaine-seeking behaviour, preventing cocaine-induced reinstatement of drug-seeking behaviour and protecting against cocaine overdose after skin transplantation, potentially making them 'immune' to further cocaine abuse. Because of the extremely high catalytic efficiency and high levels of hBChE, this approach can be highly efficient in protecting against a wide range of cocaine doses with little individual variation. It remains possible that the protective effect of *hBChE*-expressing skin grafts can be surmountable if extremely high doses of cocaine or other psychostimulants are used. For instance, it has been shown that the longer-acting mutant form of bacteria cocaine esterase can prevent cocaine-induced toxicity and ongoing intravenous self-administration in rodents, but the effects are diminished when high doses of cocaine are used[48]. Additionally, the development of drug abuse is accompanied by learned association between drug effects and environmental cues, which plays a significant role in cocaine craving and relapse[1,3,41]. Although hBChE is a highly potent cocaine hydrolase, it is unlikely to affect cue-induced relapse. It is also noteworthy that cocaine intake is not under the control of the test animals in our CPP model. Thus, future studies will be essential to determine the protective effect of hBChE, particularly in response to extremely high doses of cocaine, and to test the prevention of cue-induced relapse.

Cutaneous gene delivery with engineered epidermal stem cells may provide therapeutic opportunities for drug abuse or co-abuse beyond cocaine. For instance, glucagon-like peptide 1 (GLP1) is a major physiological incretin that controls food intake and glucose homoeostasis[49]. Several GLP1 receptor agonists have been approved by the Food and Drug Administration to treat type II diabetes. Our recent study indicates that skin-derived expression of *GLP1* can effectively correct diet-induced obesity and diabetes in mice[20]. Interestingly, GLP1 receptor agonists can also attenuate the reinforcing properties of cocaine, alcohol and nicotine in rodents[50–55]. Thus, future studies will determine whether the expression of *GLP1* from skin transplants can reduce cocaine, alcohol and nicotine use and relapse in patients with cocaine abuse, alcohol use disorder and nicotine dependence. Additionally, it will be important to investigate whether co-expression of *hBChE* and *GLP1* in skin can be used to treat alcohol and/or nicotine co-abuse with cocaine, which occurs with high frequency and significantly increases the risk of drug-related morbidity and mortality.

The immune system recognizes and reacts against foreign antigens, including those arising from gene therapy-derived products. If an immune response to these products is triggered, neutralizing antibodies are produced that prevent the function of the therapeutic molecules and may induce the rejection of the genetically modified cells[56]. Our skin transplantation model built with WT isogenic animals provides a unique approach by which to examine this process in vivo. Skin epidermal keratinocytes have low immunogenicity[30]. In the skin, Langerhans cells are the only cell type expressing *MHC* class II for antigen presentation[30], as epidermal keratinocytes are considered 'non-professional' antigen-presenting cells. Transplanted skin tissues generated from epidermal stem cells are devoid of Langerhans cells or other leukocytes with antigen presentation capabilities; therefore, the risk of antigenicity is significantly reduced. Consequently, engineered skin grafts are generally well taken and immunologically tolerated in WT isogenic animals[20–22]. Indeed, skin-derived expression of *hBChE* in host mice with intact immune systems can be stable for more than 10 wk without a significant decrease in the serum level of engineered enzyme, strongly suggesting that the low immunogenicity of the skin environment may help to reduce the antigenicity and immune reaction towards *hBChE*. Moreover, the oldest GhBChE mice are 6 months old and healthy with no tissue rejections, lending further support for the long-lasting feasibility of cutaneous gene therapy targeting cocaine abuse. Taken together, our results suggest that cutaneous gene therapy could become a potentially safe and cost-effective therapeutic option for cocaine abuse.

Methods

As the methodology of this study is similar to that in our previous work[20], text in the sections 'Reagents and plasmid DNA constructions', 'Skin organoid culture and transplantation', 'Histology and immunofluorescence', 'Cell cycle analysis' and 'Protein biochemical analysis' has been adapted from that publication.

Reagents and plasmid DNA constructions. Guinea pig anti K5, rabbit anti K14, rabbit anti K10 and loricrin antibodies were generous gifts from E. Fuchs at the Rockefeller University. Rat monoclonal β4-integrin (CD104; BD 553745) was obtained from BD Pharmingen. Ser10 pho-histone antibody was obtained from EMD Millipore. Cleaved caspase-3 antibody was obtained from Cell Signaling Technology. Rabbit polyclonal BChE antibody was obtained from Proteintech. A hBChE quantikine ELISA kit was obtained from R&D Systems. Other chemicals or reagents were obtained from Sigma, unless otherwise indicated.

The lentiviral vector encoding luciferase has been described before[21,57]. The plasmid encoding the *hCas9*^{D10A} mutant was a gift from G. Church, obtained from Addgene (plasmid number 41816). The plasmid-encoding guide RNA expression cassette was constructed with the primers AAG GAA AAA AGC GGC CGC TGT ACA AAA AAG CAG G and GGA ATT CTA ATG CCA ACT TTG TAC using gBlock as a template. The *Rosa26*-targeting guide RNA was constructed with the primers ACA CCG GCA GGC TTA AAG GCT AAC CG, AAA ACG GTT AGC CTT TAA GCC TGC CG, ACA CCG AGG ACA ACG CCC ACA CAC CG and AAA ACG GTG TGT GGG CGT TGT CCT CG. The *AAVS1*-targeting guide RNA was constructed with the primers ACA CCG TCA CCA ATC CTG TCC CTA GG, AAA ACC TAG GGA CAG GAT TGG TGA CG, ACA CCG CCC CAC AGT GGG GCC ACT AG and AAA ACT AGT GGC CCC ACT GTG GGG CG. The *Rosa26*-targeting vector was constructed with pRosa26-GT as a template (a gift from L. Luo; Addgene plasmid 40025) using the primers GAC TAG TGA ATT CGG ATC CTT AAT TAA GGC CTC CGC GCC GGG TTT TGG CG, GAC TAG TCC CGG GGG ATC CAC CGG TCA GGA ACA GGT GGT GGC GGC CC, CGG GAT CCA CCG GTG AGG GCA GAG GAA GCC TTC TAA C, TCC CCC GGG TAC AAA ATC AGA AGG ACA GGG AAG, GGA ATT CAA TAA AAT ATC TTT ATT TTC ATT ACA TC and CCT TAA TTA AGG ATC CAC GCG TGT TTA AAC ACC GGT TTT ACG AGG GTA GGA AGT GGT AC. The *AAVS1*-targeting vector was constructed with AAVS1 hPGK-PuroR-pA donor (a gift from R. Jaenisch; Addgene plasmid 22072) as a template using the primers CCC AAG CTT CTC GAG TTG GGG TTG CGC CTT TTC CAA G, CCC AAG CTT CCA TAG AGC CCA CCG CAT CCC C, CAG GGT CTA GAC GCC GGA TCC GGT ACC CTG TGC CTT CTA GTT GC, GGA TCC GGC GTC TAG ACC CTG GGG AGA GAG GTC GGT G, CCG CTC GAG AAT AAA ATA TCT TTA TTT TCA TTA CAT C and GCT CTA GAC CAA GTG ACG ATC ACA GCG ATC. The genotyping primers for CIRPSR-mediated knock-in were GAG CTG GGA CCA CCT TAT ATT C, GGT GCA TGA CCC GCA AG and GAG AGA TGG CTC CAG GAA ATG. Human and mouse *BChE* with point mutations[14] were codon optimized and synthesized from Integrated DNA Technology and PCR amplified with the primers GCT CTA GAG CCA CCA TGC AGA CTC AGC ATA CCA AGG, CGG GAT CCA CCG GTT TAG AGA GCT GTA CAA GAT TCT TTC TTG, CCC AAG CTT GCC ACC ATG CAT AGC AAA GTC ACA ATC and ACG CGT CGA CTT AGA GAC CCA CAC AAC TTT CTT TCT TG.

Skin organoid culture and transplantation. Decelluralized dermis (circular shape with 1 cm diameter) was prepared by ethylenediaminetetraacetic acid treatment of newborn mouse skin[58]. 1.5×10^6 cultured keratinocytes were seeded onto the dermis in a cell culture insert. After overnight attachment, the skin culture was exposed to air–liquid interface.

For grafting with skin organoids, CD1 or C57BL/6 males aged 6–8 wk were anaesthetized. A silicone chamber bottom with an interior diameter of 0.8 cm and exterior diameter of 1.5 cm was implanted on its shaved dorsal mid-line skin, which was used to hold the skin graft. A chamber cap was installed to seal the chamber just after a piece of graft was implanted. About 1 wk later, the chamber cap was removed to expose the graft to air. A single dose of 0.2 mg α-CD4 (GK1.5) and 0.2 mg α-CD8 (2.43.1) antibodies was administered intraperitoneally for skin grafting.

Histology and immunofluorescence. Skin or wound samples were embedded in optimal cutting temperature compound, frozen, sectioned and fixed in 4% formaldehyde. For paraffin sections, samples were incubated in 4% formaldehyde at 4 °C overnight, dehydrated with a series of increasing concentrations of ethanol and xylene, then embedded in paraffin. Paraffin sections were rehydrated in decreasing concentrations of ethanol and subjected to antigen unmasking in 10 mM citrate, pH 6.0. Sections were subjected to haematoxylin and eosin staining or immunofluorescence staining as described[59]. Antibodies were diluted according to the manufacturer's instruction, unless indicated.

Cell cycle analysis. Propidium iodide staining followed by flow cytometry assay were used to determine the effect of cell cycle profiles. Mouse and human epidermal cells were cultured in 2 6 cm cell culture dishes for 24 h, respectively. Cells were trypsinized and 1×10^5 cells from each dish were collected, followed by a phosphate buffered saline (PBS) wash. Fixation of cells was carried out using 70% (*v*/*v*) ice-cold ethanol for 1 h. Then, the fixed cells were centrifuged at 500 *g* at 4 °C for 10 min, followed by two PBS washes. The cells were then treated with 75 µg RNAse A in 100 µl PBS and incubated at 37 °C for 1 h. After incubation, the cells were collected by centrifuging at 500 *g* at 4 °C for 10 min, followed by another PBS wash. The cell pellet was re-suspended in 200 µl PBS, with the addition of propidium iodide solution at a final concentration of 25 ng µl^{-1}. After staining, the cells were analysed immediately using a BD FACSCanto II flow cytometer (BD Biosciences) with an excitation wavelength at 488 nm and emission at 585 nm. DNA content and histograms of cell cycle distribution were analysed using FlowJo software, version 10.

Protein biochemical analysis. Western blotting was performed as described previously[60]. Briefly, equal amounts of the cell lysates were separated using sodium dodecyl sulfate polyacrylamide gel electrophoresis and electroblotted onto a nitrocellulose membrane. The immunoblot was incubated with Odyssey blocking buffer (LI-COR Biosciences) at room temperature for 1 h, followed by overnight incubation with primary antibody. Blots were washed three times with Tween 20/Tris-buffered saline and incubated with a 1:10000 dilution of secondary antibody for 1 h at room temperature. Blots were washed three times with Tween 20/Tris-buffered saline again. Visualization and quantification were carried out with the LI-COR Odyssey scanner and software (LI-COR Biosciences).

Cocaine-induced behaviours. For all behavioural experiments except where noted, C57BL/6J mice were used. Roughly equal numbers of adult male and female mice were group housed until surgery. Mice were maintained under controlled temperature and humidity conditions on a 12 h:12 h light:dark cycle (lights on at 7:00). Water and food were available ad libitum. Mice weighed around 25–30 g at the beginning of the experiments. All procedures followed the National Institutes of Health Guide for the Care and Use of Laboratory Animals and were approved by the University of Chicago Institutional Animal Care and Use Committee.

Drug. Cocaine hydrochloride and methamphetamine hydrochloride (Sigma–Aldrich) were dissolved in sterile saline and delivered intraperitoneally at appropriate doses in a volume of 10 ml kg^{-1}. Ethanol (Sigma–Aldrich, 95%, density = 0.816) was prepared in 20% (*v*/*v*) diluted in sterile saline and delivered intraperitoneally at appropriate doses. Vehicle (sterile saline) was administered intraperitoneally at 10 ml kg^{-1} as a control.

Microdialysis. GhBChE and GWT mice were anaesthetized with isofluorane and placed in a flat skull position in a Kopf stereotaxic frame. A guide cannula was secured with dental cement on the mouse skulls above the nucleus accumbens using the anterior–posterior + 1.2 mm, medial–lateral 1.0 mm and dorsal–ventral −5.0 mm from the bregma coordinates. Then, 24 h after implantation, a microdialysis probe (2 mm dialysing membrane, CMA-7; Harvard Apparatus) was inserted into the guide cannula and lowered down to the nucleus accumbens region in freely moving mice. The microdialysis probe was flushed with artificial cerebrospinal fluid (KCl 2.5 mM, NaCl 125 mM, $CaCl_2$ 1.26 mM, $MgCl_2$ 1.18 mM, Na_2HPO_4 2 mM, pH 7.4) at a flow rate of 1 µl min^{-1} using a UMP3 UltraMicroPump (World Precision Instruments). Once the probe was positioned, it was flushed at 1 µl min^{-1} for 140 min. Dialysates were collected at 20 min intervals. 10 µl dialysate was derivatized using BzCl for the analysis of extracellular dopamine. Another 10 µl dialysate without derivatization was used for the analysis of cocaine. Dopamine-1,1,2,2-d4 and Cocaine-d3 were used as internal standards. At the completion of the experiment, mice were euthanized and probe placement was confirmed with histology (Supplementary Fig. 2d).

LC-MS analysis. We used a method by Wong et al.[42]. Derivatized dialysate samples were analysed by LC-MS using an Agilent 1290 UHPLC system coupled to a 6460 triple quadrupole mass spectrometer in multiple reaction monitoring mode. Samples of 5 µl were injected onto an InfinityLab Poroshell 120 EC-C18 (2.1 mm × 100 mm, 4 µm, 100 Å pore size). Samples were analysed in triplicate. Electrospray ionization was used in positive mode. Automated peak integration was performed using Agilent MassHunter Workstation Quantitative Analysis for QQQ. All peaks were visually inspected to ensure proper integration.

Acetylcholine assay. The baseline level of acetylcholine in the blood serum of GhBChE and GWT mice was quantified using a QuickDetect Acetylcholine (Mouse) ELISA kit. A standard curve was generated using known concentrations of standard mouse acetylcholine and its corresponding optical density value. 10 µl of blood serum collected before cocaine injection was diluted with a 40 µl sample dilution buffer (a dilution factor of 5). The acetylcholine concentration was determined following the manufacturer-recommended protocol.

Acute locomotor activity. Baseline motor activity and locomotor responses to cocaine were assessed using horizontal arenas equipped with infrared detectors[61]. Mice were habituated in the test chambers for 1 h before testing. Mice were then given an intraperitoneal (i.p.) injection of cocaine at three different doses (10, 20 and 40 mg kg^{-1}) or saline. Their locomotor responses (distance travelled and stereotypical behaviours) were recorded for another hour after the injections.

CPP apparatus. The CPP apparatus (Med Associates) consisted of two larger chambers (16.8 cm × 12.7 cm × 12.7 cm), which were separated by a smaller chamber (7.2 cm × 12.7 cm × 12.7 cm) as previously described[44]. Each chamber had a unique combination of visual and tactile properties (one large chamber had black walls and a rod floor, the other large chamber had white walls with a mesh floor and the middle chamber had grey walls and a solid grey floor). Each compartment had a light embedded in a clear, Plexiglas hinged lid. Time spent in each chamber was measure via photobeam breaks and recorded. The CPP was determined on testing days via time spent in the drug-paired side minus time spent in the saline-paired side.

Acquisition of CPP. We used a biased CPP procedure similar to that from a previous study in our laboratory[44]. Acquisition of CPP consisted of three sequential procedures—pre-testing, conditioning and testing. After 7–12 d of recovery from engrafting surgeries, mice underwent pre-testing on day 1, where mice were allowed to freely explore the entire chamber for 20 min once daily. Mice that spent more than 500 s in the grey compartment or more than 800 s in either of the large compartments were excluded from the study. Following the pre-test day, mice underwent conditioning and testing on days 2–5. Starting on day 2, mice received an i.p. injection of drug (10 mg kg^{-1} cocaine in cocaine CPP or 2 g kg^{-1} ethanol in ethanol CPP) and were confined to the white chamber for 30 min. At least 5 h afterwards on the same day, mice received an i.p. injection of saline and were confined to the black compartment for 30 min. On day 6 (the test day) mice were allowed to explore the entire chambers for 20 min and the time spent in each area was recorded.

Extinction and reinstatement of CPP. Following CPP acquisition, mice underwent extinction, the procedure for which was identical to that on the test day. On each extinction day, mice were allowed to explore the entire chambers for 20 min and the time spent in each area was recorded. Extinction was performed until the CPP decreased to a level that was not different from that of the pre-test on two consecutive days. On the following day of the last extinction, mice underwent reinstatement procedures, in which mice that were trained for cocaine CPP received an i.p. injection of 15 mg kg^{-1} cocaine, and mice that were trained for ethanol CPP received an i.p. injection of 1 g kg^{-1} ethanol. Immediately following injection, mice were allowed to explore the entire chambers for 20 min and the time spent in each area was recorded.

Acute drug overdose test. Two weeks after grafting surgery, 4 groups of GhBChE and 4 groups of GWT mice ($n = 8$ in each group) received i.p. injections of cocaine at 40, 80, 120 and 160 mg kg^{-1}. As a control, 4 groups of GhBChE and 4 groups of GWT mice ($n = 8$ in each group) received i.p. injections of methamphetamine at 34, 68 (LD50), 100 and 160 mg kg^{-1}. Two each of GhBChE and GWT mice with CD1 mice as hosts were also used to videotape acute (80 mg kg^{-1}) cocaine-induced behaviours. Mice were monitored for 2 h following injection and the percent cocaine- and methamphetamine-induced lethality was calculated.

Specific methods. Figure 3a: one group of GhBChE and one group of GWT mice ($n = 9$ in each group) were trained for cocaine CPP 7 d after engraftment. Mice underwent pre-testing on day 1, 4 d of cocaine conditioning from day 2 to day 5, and CPP testing on day 6. Figure 3b: one group of GhBChE and one group of GWT mice ($n = 8$ in each group) were trained for ethanol CPP 7 d after engraftment. Mice underwent pre-testing on day 1, 4 d of ethanol conditioning from day 2 to day 5, and CPP testing on day 6. Figure 3c: two groups of drug-naïve WT mice ($n = 8$ in each group) were trained for cocaine CPP from day 1 to day 6. On the following day, mice underwent engrafting surgery. The behavioural procedure resumed after engraftment surgery from day 18. Extinction was performed from day 18 to day 31. On day 32, mice underwent reinstatement induced by i.p. injection of cocaine. Figure 3d: one group of GhBChE and one group of GWT mice ($n = 8$ in each group) were trained for ethanol CPP from day 1 to day 6. Extinction was performed from day 7 to day 20. On day 21, mice underwent reinstatement induced by i.p. injection of ethanol.

Statistical analysis. Statistical analysis was performed using Excel or OriginLab software. Box plots are used to describe the entire population without assumptions on the statistical distribution. A Student's *t*-test was used to assess the statistical significance (*P* value) of differences between two experimental conditions. For cocaine behavioural analysis, CPP results were analysed using repeated-measures ANOVA with within factor time (testing days) and between factor treatment (engraftment). Significant effects were further analysed with Fisher's *t*-tests.

Reporting Summary. Further information on research design is available in the Nature Research Reporting Summary linked to this article.

Data availability

The authors declare that all data supporting the findings of this study are available within the paper and its Supplementary Information. Source data for Figs. 2 and 3 are available in Figshare at https://figshare.com/s/898c3ab26b10a3d08b13.

Received: 14 September 2017; Accepted: 15 August 2018;
Published online: 17 September 2018

References

1. Kalivas, P. W. & O'Brien, C. Drug addiction as a pathology of staged neuroplasticity. *Neuropsychopharmacology* **33**, 166–180 (2008).
2. Koob, G. F. & Volkow, N. D. Neurobiology of addiction: a neurocircuitry analysis. *Lancet Psychiatry* **3**, 760–773 (2016).
3. O'Brien, C. P., Childress, A. R., Ehrman, R. & Robbins, S. J. Conditioning factors in drug abuse: can they explain compulsion? *J. Psychopharmacol.* **12**, 15–22 (1998).
4. Heard, K., Palmer, R. & Zahniser, N. R. Mechanisms of acute cocaine toxicity. *Open Pharmacol. J.* **2**, 70–78 (2008).
5. Zimmerman, J. L. Cocaine intoxication. *Crit. Care Clin.* **28**, 517–526 (2012).
6. Brimijoin, S. Interception of cocaine by enzyme or antibody delivered with viral gene transfer: a novel strategy for preventing relapse in recovering drug users. *CNS Neurol. Disord. Drug Targets* **10**, 880–891 (2011).
7. Lockridge, O. Review of human butyrylcholinesterase structure, function, genetic variants, history of use in the clinic, and potential therapeutic uses. *Pharmacol. Ther.* **148**, 34–46 (2015).
8. Schindler, C. W. & Goldberg, S. R. Accelerating cocaine metabolism as an approach to the treatment of cocaine abuse and toxicity. *Future Med. Chem.* **4**, 163–175 (2012).
9. Murthy, V. et al. Reward and toxicity of cocaine metabolites generated by cocaine hydrolase. *Cell. Mol. Neurobiol.* **35**, 819–826 (2015).
10. Sun, H. et al. Predicted Michaelis–Menten complexes of cocaine-butyrylcholinesterase. Engineering effective butyrylcholinesterase mutants for cocaine detoxication. *J. Biol. Chem.* **276**, 9330–9336 (2001).
11. Sun, H., Pang, Y. P., Lockridge, O. & Brimijoin, S. Re-engineering butyrylcholinesterase as a cocaine hydrolase. *Mol. Pharmacol.* **62**, 220–224 (2002).
12. Xue, L. et al. Catalytic activities of a cocaine hydrolase engineered from human butyrylcholinesterase against (+)- and (−)-cocaine. *Chem. Biol. Interact.* **203**, 57–62 (2013).
13. Zheng, F. et al. Most efficient cocaine hydrolase designed by virtual screening of transition states. *J. Am. Chem. Soc.* **130**, 12148–12155 (2008).
14. Zheng, F. et al. A highly efficient cocaine-detoxifying enzyme obtained by computational design. *Nat. Commun.* **5**, 3457 (2014).
15. Connors, N. J. & Hoffman, R. S. Experimental treatments for cocaine toxicity: a difficult transition to the bedside. *J. Pharmacol. Exp. Ther.* **347**, 251–257 (2013).
16. Cohen-Barak, O. et al. Safety, pharmacokinetics, and pharmacodynamics of TV-1380, a novel mutated butyrylcholinesterase treatment for cocaine addiction, after single and multiple intramuscular injections in healthy subjects. *J. Clin. Pharmacol.* **55**, 573–583 (2015).
17. Gilgun-Sherki, Y. et al. Placebo-controlled evaluation of a bioengineered, cocaine-metabolizing fusion protein, TV-1380 (AlbuBChE), in the treatment of cocaine dependence. *Drug Alcohol Depend.* **166**, 13–20 (2016).
18. Kotterman, M. A., Chalberg, T. W. & Schaffer, D. V. Viral vectors for gene therapy: translational and clinical outlook. *Annu. Rev. Biomed. Eng.* **17**, 63–89 (2015).
19. Naldini, L. Gene therapy returns to centre stage. *Nature* **526**, 351–360 (2015).
20. Yue, J., Gou, X., Li, Y., Wicksteed, B. & Wu, X. Engineered epidermal progenitor cells can correct diet-induced obesity and diabetes. *Cell Stem Cell.* **21**, 256–263 (2017).
21. Liu, H. et al. Regulation of focal adhesion dynamics and cell motility by the EB2 and Hax1 protein complex. *J. Biol. Chem.* **290**, 30771–30782 (2015).
22. Yue, J. et al. In vivo epidermal migration requires focal adhesion targeting of ACF7. *Nat. Commun.* **7**, 11692 (2016).
23. Rasmussen, C., Thomas-Virnig, C. & Allen-Hoffmann, B. L. Classical human epidermal keratinocyte cell culture. *Methods Mol. Biol.* **945**, 161–175 (2013).
24. Rheinwald, J. G. & Green, H. Serial cultivation of strains of human epidermal keratinocytes: the formation of keratinizing colonies from single cells. *Cell* **6**, 331–343 (1975).
25. Rheinwald, J. G. & Green, H. Epidermal growth factor and the multiplication of cultured human epidermal keratinocytes. *Nature* **265**, 421–424 (1977).
26. Blanpain, C. & Fuchs, E. Epidermal stem cells of the skin. *Annu. Rev. Cell. Dev. Biol.* **22**, 339–373 (2006).
27. Watt, F. M. Mammalian skin cell biology: at the interface between laboratory and clinic. *Science* **346**, 937–940 (2014).
28. Carsin, H. et al. Cultured epithelial autografts in extensive burn coverage of severely traumatized patients: a five year single-center experience with 30 patients. *Burns* **26**, 379–387 (2000).
29. Coleman, J. J. 3rd & Siwy, B. K. Cultured epidermal autografts: a life-saving and skin-saving technique in children. *J. Pediatr. Surg.* **27**, 1029–1032 (1992).
30. Haniffa, M., Gunawan, M. & Jardine, L. Human skin dendritic cells in health and disease. *J. Dermatol. Sci.* **77**, 85–92 (2015).
31. Christensen, R., Jensen, U. B. & Jensen, T. G. Skin genetically engineered as a bioreactor or a 'metabolic sink'. *Cells Tissues Organs* **172**, 96–104 (2002).
32. Del Rio, M., Gache, Y., Jorcano, J. L., Meneguzzi, G. & Larcher, F. Current approaches and perspectives in human keratinocyte-based gene therapies. *Gene Ther.* **11**, S57–S63 (2004).
33. Fakharzadeh, S. S., Zhang, Y., Sarkar, R. & Kazazian, H. H. Jr. Correction of the coagulation defect in hemophilia A mice through factor VIII expression in skin. *Blood* **95**, 2799–2805 (2000).
34. Fenjves, E. S., Gordon, D. A., Pershing, L. K., Williams, D. L. & Taichman, L. B. Systemic distribution of apolipoprotein E secreted by grafts of epidermal keratinocytes: implications for epidermal function and gene therapy. *Proc. Natl Acad. Sci. USA* **86**, 8803–8807 (1989).
35. Gerrard, A. J., Hudson, D. L., Brownlee, G. G. & Watt, F. M. Towards gene therapy for haemophilia B using primary human keratinocytes. *Nat. Genet.* **3**, 180–183 (1993).
36. Morgan, J. R., Barrandon, Y., Green, H. & Mulligan, R. C. Expression of an exogenous growth hormone gene by transplantable human epidermal cells. *Science* **237**, 1476–1479 (1987).
37. Ran, F. A. et al. Double nicking by RNA-guided CRISPR Cas9 for enhanced genome editing specificity. *Cell* **154**, 1380–1389 (2013).
38. Chen, X. et al. Kinetic characterization of a cocaine hydrolase engineered from mouse butyrylcholinesterase. *Biochem. J.* **466**, 243–251 (2015).
39. Schober, M. & Fuchs, E. Tumor-initiating stem cells of squamous cell carcinomas and their control by TGF-beta and integrin/focal adhesion kinase (FAK) signaling. *Proc. Natl Acad. Sci. USA* **108**, 10544–10549 (2011).
40. Sebastiano, V. et al. Human COL7A1-corrected induced pluripotent stem cells for the treatment of recessive dystrophic epidermolysis bullosa. *Sci. Transl. Med.* **6**, 264ra163 (2014).
41. Koob, G. F. & Volkow, N. D. Neurocircuitry of addiction. *Neuropsychopharmacology* **35**, 217–238 (2010).
42. Wong, J. M. et al. Benzoyl chloride derivatization with liquid chromatography–mass spectrometry for targeted metabolomics of neurochemicals in biological samples. *J. Chromatogr. A* **1446**, 78–90 (2016).
43. Cunningham, C. L., Gremel, C. M. & Groblewski, P. A. Drug-induced conditioned place preference and aversion in mice. *Nat. Protoc.* **1**, 1662–1670 (2006).
44. Yan, Y., Kong, H., Wu, E. J., Newman, A. H., & Xu, M. Dopamine D3 receptors regulate reconsolidation of cocaine memory. *Neuroscience* **241**, 32–40 (2013).
45. Still, J. M. Jr, Orlet, H. K. & Law, E. J. Use of cultured epidermal autografts in the treatment of large burns. *Burns* **20**, 539–541 (1994).
46. Guerra, L. et al. Treatment of 'stable' vitiligo by timedsurgery and transplantation of cultured epidermal autografts. *Arch. Dermatol.* **136**, 1380–1389 (2000).
47. Shinkuma, S. et al. Long-term follow-up of cultured epidermal autograft in a patient with recessive dystrophic epidermolysis bullosa. *Acta Derm. Venereol.* **94**, 98–99 (2014).
48. Collins, G. T. et al. Cocaine esterase prevents cocaine-induced toxicity and the ongoing intravenous self-administration of cocaine in rats. *J. Pharmacol. Exp. Ther.* **331**, 445–455 (2009).
49. Sandoval, D. A. & D'Alessio, D. A. Physiology of proglucagon peptides: role of glucagon and GLP-1 in health and disease. *Physiol. Rev.* **95**, 513–548 (2015).
50. Egecioglu, E. et al. The glucagon-like peptide 1 analogue exendin-4 attenuates alcohol mediated behaviors in rodents. *Psychoneuroendocrinology* **38**, 1259–1270 (2013).
51. Shirazi, R. H., Dickson, S. L. & Skibicka, K. P. Gut peptide GLP-1 and its analogue, exendin-4, decrease alcohol intake and reward. *PLoS ONE* **8**, e61965 (2013).
52. Skibicka, K. P. The central GLP-1: implications for food and drug reward. *Front. Neurosci.* **7**, 181 (2013).
53. Sorensen, G., Caine, S. B. & Thomsen, M. Effects of the GLP-1 agonist exendin-4 on intravenous ethanol self-administration in mice. *Alcohol. Clin. Exp. Res.* **40**, 2247–2252 (2016).
54. Sorensen, G. et al. The glucagon-like peptide 1 (GLP-1) receptor agonist exendin-4 reduces cocaine self-administration in mice. *Physiol. Behav.* **149**, 262–268 (2015).
55. Vallof, D. et al. The glucagon-like peptide 1 receptor agonist liraglutide attenuates the reinforcing properties of alcohol in rodents. *Addict. Biol.* **21**, 422–437 (2016).

56. Collins, M. & Thrasher, A. Gene therapy: progress and predictions. *Proc. Biol Sci.* **282**, 20143003 (2015).
57. Yue, J. et al. In vivo epidermal migration requires focal adhesion targeting of ACF7. *Nat. Commun.* **7**, 11692 (2016).
58. Prunieras, M., Regnier, M. & Woodley, D. Methods for cultivation of keratinocytes with an air–liquid interface. *J. Invest. Dermatol.* **81**, 28s–33s (1983).
59. Guasch, G. et al. Loss of TGFbeta signaling destabilizes homeostasis and promotes squamous cell carcinomas in stratified epithelia. *Cancer Cell* **12**, 313–327 (2007).
60. Wu, X., Suetsugu, S., Cooper, L. A., Takenawa, T. & Guan, J. L. Focal adhesion kinase regulation of N-WASP subcellular localization and function. *J. Biol. Chem.* **279**, 9565–9576 (2004).
61. Xu, M. et al. Elimination of cocaine-induced hyperactivity and dopamine-mediated neurophysiological effects in dopamine D1 receptor mutant mice. *Cell* **79**, 945–955 (1994).

Acknowledgements

We are very grateful to L. Becker and X. Zhuang at the University of Chicago, M. Schober at New York University School of Medicine, and E. Fuchs at the Rockefeller University for sharing reagents and technical assistance. We thank L. Degenstein at the transgenic core facility at the University of Chicago for excellent technical assistance. We thank M. Roitman at the University of Illinois at Chicago for advice on dopamine measurements. The animal studies were carried out in the Animal Lovers Against Animal Cruelty-accredited animal research facility at the University of Chicago. This work was supported by grants NIH R01AR063630 and R01OD023700, the Research Scholar Grant (RSG-13-198-01) from the American Cancer Society, and the V Scholar Award from the V Foundation to X.W., and by NIH DA036921, DA043361 and CTSA UL1 TR000430 to M.X.

Author contributions

X.W. and M.X. designed the experiments. Y.L., Q.K., J.Y. and X.G. performed the experiments. Y.L., Q.K., J.Y., M.X. and X.W. analysed the data. X.W. and M.X. wrote the manuscript. All authors edited the manuscript.

Competing interests

The authors declare no competing interests.

Additional information

Supplementary information is available for this paper at https://doi.org/10.1038/s41551-018-0293-z.

Reprints and permissions information is available at www.nature.com/reprints.

Correspondence and requests for materials should be addressed to M.X. or X.W.

Publisher's note: Springer Nature remains neutral with regard to jurisdictional claims in published maps and institutional affiliations.

nature research

Corresponding author(s): Xiaoyang Wu

Reporting Summary

Nature Research wishes to improve the reproducibility of the work that we publish. This form provides structure for consistency and transparency in reporting. For further information on Nature Research policies, see Authors & Referees and the Editorial Policy Checklist.

Statistical parameters

When statistical analyses are reported, confirm that the following items are present in the relevant location (e.g. figure legend, table legend, main text, or Methods section).

n/a	Confirmed	
☐	☒	The exact sample size (*n*) for each experimental group/condition, given as a discrete number and unit of measurement
☐	☒	An indication of whether measurements were taken from distinct samples or whether the same sample was measured repeatedly
☐	☒	The statistical test(s) used AND whether they are one- or two-sided *Only common tests should be described solely by name; describe more complex techniques in the Methods section.*
☐	☒	A description of all covariates tested
☐	☒	A description of any assumptions or corrections, such as tests of normality and adjustment for multiple comparisons
☐	☒	A full description of the statistics including central tendency (e.g. means) or other basic estimates (e.g. regression coefficient) AND variation (e.g. standard deviation) or associated estimates of uncertainty (e.g. confidence intervals)
☐	☒	For null hypothesis testing, the test statistic (e.g. *F*, *t*, *r*) with confidence intervals, effect sizes, degrees of freedom and *P* value noted *Give P values as exact values whenever suitable.*
☐	☒	For Bayesian analysis, information on the choice of priors and Markov chain Monte Carlo settings
☐	☒	For hierarchical and complex designs, identification of the appropriate level for tests and full reporting of outcomes
☐	☒	Estimates of effect sizes (e.g. Cohen's *d*, Pearson's *r*), indicating how they were calculated
☐	☒	Clearly defined error bars *State explicitly what error bars represent (e.g. SD, SE, CI)*

Our web collection on statistics for biologists may be useful.

Software and code

Policy information about availability of computer code

Data collection	Flowjo, Version 10.
Data analysis	Excel 2010, originlab 2016, flowjo version 10.

For manuscripts utilizing custom algorithms or software that are central to the research but not yet described in published literature, software must be made available to editors/reviewers upon request. We strongly encourage code deposition in a community repository (e.g. GitHub). See the Nature Research guidelines for submitting code & software for further information.

Data

Policy information about availability of data

All manuscripts must include a data availability statement. This statement should provide the following information, where applicable:

- Accession codes, unique identifiers, or web links for publicly available datasets
- A list of figures that have associated raw data
- A description of any restrictions on data availability

The authors declare that all data supporting the findings of this study are available within the paper and its supplementary information. Source data for Figures 2 and 3 are available in Figshare: https://figshare.com/s/898c3ab26b10a3d08b13 (ref. 63).

Field-specific reporting

Please select the best fit for your research. If you are not sure, read the appropriate sections before making your selection.

☒ Life sciences ☐ Behavioural & social sciences ☐ Ecological, evolutionary & environmental sciences

For a reference copy of the document with all sections, see nature.com/authors/policies/ReportingSummary-flat.pdf

Life sciences study design

All studies must disclose on these points even when the disclosure is negative.

Sample size	Based on mean and standard deviation data from our previous studies, a biostatistician, Kristin Wroblewski, from the Biostatistics Core at the Department of Health at our university, performed a sample-size determination for the project.
Data exclusions	No data were excluded.
Replication	Experiments were reliably reproduced.
Randomization	For test animals, we used the same C57Bl/6j or CD1 mice at a similar age. Roughly equal numbers of adult male and female mice were used in the analysis. Animals were randomly allocated to the experimental groups.
Blinding	Transplanted mice were blind to investigators performing the experiments until data analysis was completed.

Reporting for specific materials, systems and methods

Materials & experimental systems

n/a	Involved in the study
☒	☐ Unique biological materials
☐	☒ Antibodies
☐	☒ Eukaryotic cell lines
☒	☐ Palaeontology
☐	☒ Animals and other organisms
☒	☐ Human research participants

Methods

n/a	Involved in the study
☒	☐ ChIP-seq
☐	☒ Flow cytometry
☒	☐ MRI-based neuroimaging

Antibodies

Antibodies used	Antibody used: Guinea pig anti-K5 (gift from Dr. Elaine Fuchs), rabbit anti-K14, anti-K10 and loricrin antibody (gifts from Dr. Elaine Fuchs). Anti-beta4-integrin (Rat monoclonal, BD 553745, from BD Pharmigen). Ser Pho-histone antibody (EMD Millipore). Cleaved caspase 3: cell signaling technology, BChE antibody: Proteintech.
Validation	All antibodies were validated by immunoblots or immuofluorescence stainings with proper negative controls to detect mouse and human proteins.

Eukaryotic cell lines

Policy information about cell lines

Cell line source(s)	Mouse primary keratinocytes were isolated from newborn mouse skin. Human newborn keratinocytes were purchased from Invitrogen/Life Science.
Authentication	Only primary cells were used. No authentication was used.
Mycoplasma contamination	All the cells were tested and determined not to be contaminated with mycoplasma.
Commonly misidentified lines (See ICLAC register)	No commonly misidentified cell lines were used in this study.

Animals and other organisms

Policy information about studies involving animals; ARRIVE guidelines recommended for reporting animal research

Laboratory animals	Roughly equal numbers of adult male and female (CD1 or C57/B6) mice were used.
Wild animals	The study did not involve wild animals
Field-collected samples	The study did not involve samples collected from the field.

Flow Cytometry

Plots

Confirm that:

☒ The axis labels state the marker and fluorochrome used (e.g. CD4-FITC).

☒ The axis scales are clearly visible. Include numbers along axes only for bottom left plot of group (a 'group' is an analysis of identical markers).

☐ All plots are contour plots with outliers or pseudocolor plots.

☒ A numerical value for number of cells or percentage (with statistics) is provided.

Methodology

Sample preparation	Propidium Iodide (PI) staining followed by Flow Cytometry Assay were used to determine the effect of cell-cycle profiles. Mouse and human epidermal cells were cultured in two 6-cm cell-culture dishes for 24 hours, respectively. Cells were trypsinized and 1×10^5 cells from each dish were collected, followed by one PBS wash. Fixation of cells was carried out using 70% (v/v) ice cold ethanol for 1 hour. Then, the fixed cells were centrifuged at 500 g at 4 oC for 10 minutes, followed by PBS wash for two times. The cells were then treated with 75 µg RNAse A in 100 µl PBS and incubated at 37 oC for 1 hour. After incubation, the cells were collected by centrifuging at 500 g at 4 oC for 10 minutes, followed by another PBS wash. The cell pellet was re-suspended in 200 µl PBS, in addition of PI solution at a final concentration of 25 ng/µl. After staining, the cells were analyzed immediately using flow cytometer BD FACSCantoTM II (BD Biosciences, San Jose, CA) with an excitation wavelength at 488 nm and emission at 585 nm.
Instrument	BD FACSCantoTM II (BD Biosciences, San Jose, CA)
Software	FlowJo software, version 10
Cell population abundance	FACS was used to assess cell-cycle profile for purified skin keratinocytes.
Gating strategy	Gating was determined by using non-PI stained cells as negative control.

☐ Tick this box to confirm that a figure exemplifying the gating strategy is provided in the Supplementary Information.